PROCEEDINGS, 48th Workshop on Geothermal Reservoir Engineering
Stanford University, Stanford, California, February 6-8, 2023
SGP-TR-224

Geostatistical Simulation of Reservoir Convection Indicators in Ďurkov Hydrogeothermal Structure (Slovakia)

Ladislav Vizi[1], Branislav Fričovský[2]

1) Dept. 3D/4D of Geological Modelling, State Geological Institute of Dionýz Štúr, Jesenskeho 8, 04001 Košice, Slovakia

2) Dept. of Hydrogeology and Geothermal Energy, State Geological Institute of Dionýz Štúr, Mlynská dolina 1, 81704 Bratislava, Slovakia

ladislav.vizi@geology.sk

Keywords: convection indicators, reservoir modelling, geostatistics, simulation, volumetrics

ABSTRACT

Since pioneering exploration in the '70s and following hydrogeothermal evaluation in the '90s, the Ďurkov hydrogeothermal structure is considered amongst the most prospective geothermal water bodies in Slovakia. The geothermal resources were definitely proven in 1999 through the realisation of 3 geothermal wells, GTD-1 to GTD-3, quantifying 42 MWt for free-flow and 92 MWt for pumping strategy. The resource is geothermal water at up to 180 °C and moderate-high thermodynamic quality in the deepest parts of the system. Although numerous plans for production exist, there is no project online at the site yet. Reservoir characterization using a combination of geothermal techniques and geostatistical modelling tools have been used to produce a realistic 3D reservoir model consisting of the simulated convention indicators. Geostatistical simulations have become very popular in different areas of spatial modelling for spatial simulation of properties, geometries or heterogeneities. The geostatistical approach is supportive of the quantification and interpretation of possible convection formation, necessary to understand reservoir engineering and construction of reservoir prediction and response models. Turning band method of the spatial simulation was used to create multiple realisations of selected convection indicators within the reservoir body due to evident non-stationary behaviour in the vertical direction. Turning band simulations were conditioned by universal kriging using modelled directional variograms of the global trend residuals with respective drift functions for each studied convection indicator. The volumetric curves were derived from final numerical models and probable volumes above the indicator thresholds were calculated and visualised. Based on simulations carried out, the possibility of isolated convection cells has been identified in deeper parts of a system, not exposed to any bifurcation or a phase change. Limited heat and mass flux explain the observed overheating ratio distribution, implying weak breaks of generally diffuse, conduction-dominated geothermal profile in a reservoir body.

1. INTRODUCTION

All common definitions refer the geothermal energy as to the heat of the Earth. A non-disturbed vertical temperature distribution following the thermal gradient characterizes the *conductive environment* (Ledru & Gillou-Frottier, 2010), while systems encountering perturbations to the stable thermal profile define the *convective environment* (Kühn et al., 2006) due to the heat and mass fluxes consequent to a non-uniform heat source or reservoir media density gradients. The convection as a process of energy and mass transport within geothermal systems contributes at various scales in controls on energy balance, boiling, (re)equilibration at water-rock interface, or moderates an impact of thermal breakthrough (e.g. Bodvarsson et al., 1982; Toth, 2012; Wang a Horne, 2000). Although reservoir convection cannot be measured directly, several methods to analyse its plausibility and magnitude have already been introduced into a praxis. Amongst them, the numerical indices are applied mainly. Comparison between the actual Rayleigh number *Ra* and critical Rayleigh number *Rc* forms a basis of the linear stability analysis. General agreement exists that the convection sets on if $Ra \geq Rc$ (Kassoy & Zebib, 1975).In general the rule is valid for horizontally bedded and uniformly heated media. If the latter does not apply, the rule is valid no more as long as the correction by the overheat ratio τ is not included in the *Rc* calculation (Hanano, 1998).

Geostatistical simulations have become very popular for a spatial simulation of studied reservoir properties and processes as well as to solve many others problems related to the subsurface reservoir engineering (Vidal and Archer, 2015). Geostatistical simulation is a process of generating of one realisation from all possible realisations at a given point or within a volume (Ravenscroft, 1994). Unlike the traditional deterministic methods of spatial interpolations, that always give a unique solution in sense of input parameters, the geostatistical simulations represent a set of possible versions of the reality, coherent with the input data values and a used model of variability. Each realisation also replicates the statistical and spatial characteristics of the input data. The set of the realisations constitutes a numerical model with a range of possible values at any location within a studied domain and thus it provides a distribution of the values for each location. These distributions of the numerical model are basis for different risk analyses, decision-making or uncertainty evaluation. For instance, a numerical model can be used to answer different questions as "What is probability to exceed overheating ratio equal to 0.2?" or "What is a mean value of overheating ratio values above 0.2?" etc. Traditional estimation techniques do not provide a correct answer.

The Ďurkov hydrogeothermal structure represents a depressed morphostructure of Mesozoic carbonates beneath Neogene sedimentary basin fill of the Košice Depression, which is the northward promontory of the Pannonian Basin (Pereszlenyi et al., 1999). Limits are set along tectonic margins with the neovolcanic Slanské vrchy Mts. to the east, Bidovce depression on the north and west, and the W–E faults on the south, where carbonate blocks elevate nearby Vyšný Čaj (Fig 1). The deep geological structure reflects a typical vertical profile of

Neogene sedimentary basins in the Western Carpathians. Quaternary accumulations (fluvial, proluvial and deluvial forms) are only several meters thick; thus are neglected in the deep structural models.

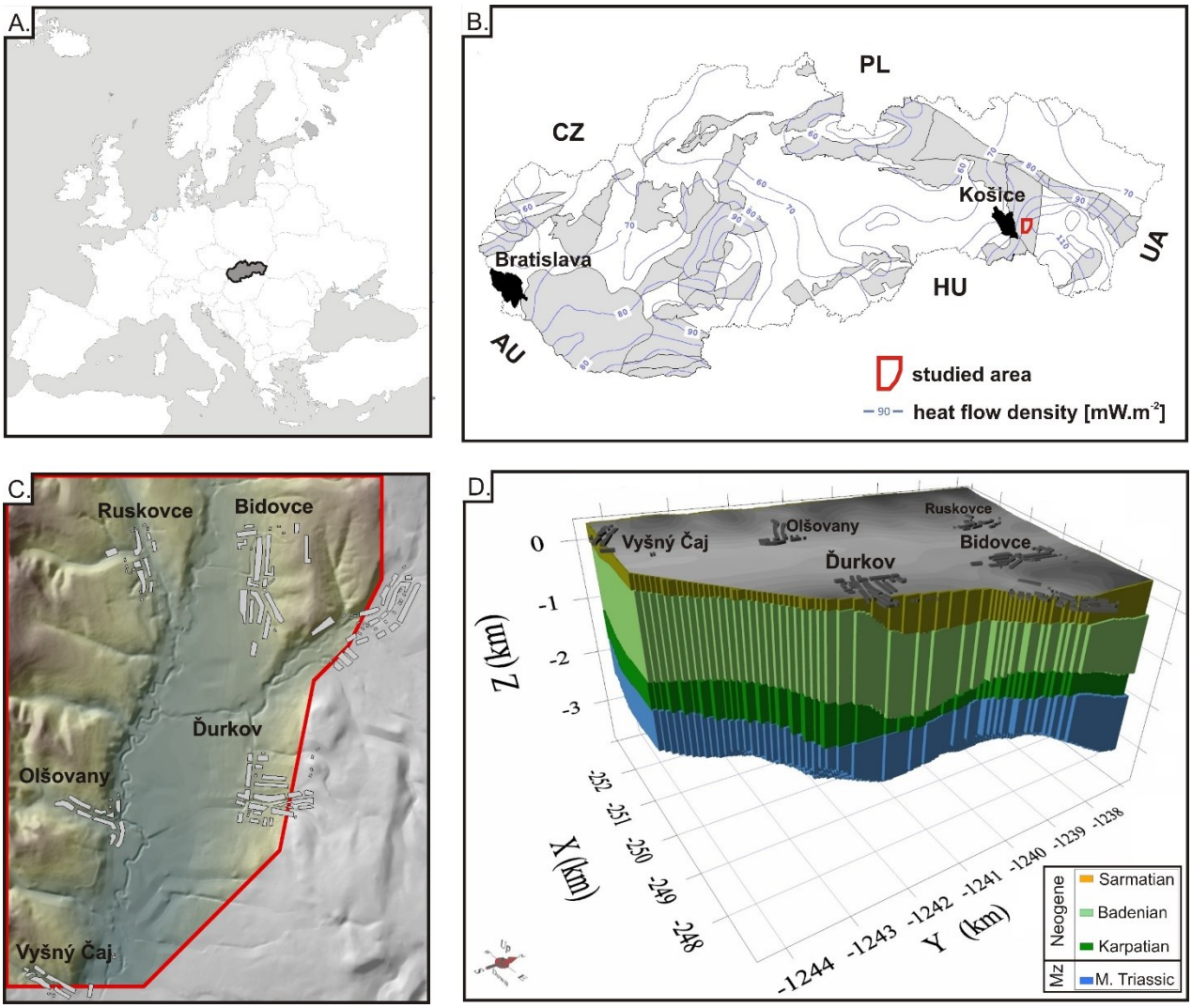

Figure 1: Ďurkov hydrothermal structure localization map and geological model.

Neogene profile thickness reaches up to 1,600 – 2,600 m. It consists of siliciclastic formations with variable contribution of sandstones and claystones, occasionally intercalated with evaporates in basal Karpatian profile, where also conglomerates and dolomitic breccia occur (Pereszlenyi et al., 1999). The Middle Triassic carbonates form a primary reservoir body, increasing in thickness in the NW–SE and SW–NE direction from 200 to 2,200 m. A very few is known about pre-Mesozoic underbed, however, analogously to the Western Carpathians, crystalline complex (magmatites and metamorphites) of the Veporic unit is expected instantly beneath (Pereszlenyi et al., 1999).

The structure is repeatedly considered amongst the most prospective in the country, with highest sampled reservoir (Tres = 150 °C) and wellhead (Twh = 135 °C) temperatures. Models on thermodynamic parameters (Fričovský et al., 2018) assume moderate thermodynamic quality and a single phase, saturated fluid as a resource at natural conditions. However, questions arise on the existence of a gaseous cap at a top of the reservoir documented by sampling high CO_2 fluxes. Analysis of convection plausibility may, thus, help answering a problem of an origin of the phase, as well as can contribute on general understanding of hydrogeothermal systems, generally referred as conductive-only.

The aim of the paper is application of geostatistical modelling and stochastic simulation to identify a possibility of isolated convection cells within the Ďurkov hydrogeothermal structure in sense of spatial modelling of the convention indicators like Rayleigh number and overheating ratio. Geostatistical simulations are used to model probability to obtain positive values of differences between calculated Rayleigh number and critical Rayleigh number as well as probability of getting overheating ratio values above 200.

2. GEOSTATISTICAL MODELLING

Geostatistics is a rapidly evolving scientific branch of applied statistics and mathematics that studies the spatial-temporal phenomena and thus extends the concept of traditional statistical methods of data processing in a spatial form. It was originally developed by George Matheron of Centre de Morphologie Mathématique in France for solving the problems of the ore reserve estimation in the mining industry but it is nowadays very popular not only in geology but also in many other areas of the natural science. Spatial data, in the framework of geosciences, exhibit some degree of spatial correlation, which is a function of the distance – the greater the distance between samples, the lower the similarity between the data, but on the contrary, the higher is their variability (Matheron, 1963). The paper does not intend to present a deep review of geostatistics with all its algorithms and methods. A number of geostatictical books are available that document the principles, methods and techniques, include for instance Journel and Huijbregts (1978), Isaaks and Srivastava (1989), Clark and Harper (2000), Armstrong (1998), Goovaerts (1997), Webster and Oliver (2001), Wackernagel (2003), Chilès and Delfiner (2000), Olea (1999), Lantuéjoul (2002), Leuangthong et al. (2008) etc, Tonnes of notes, courses and papers that have been published to study the topic. Since its definition in 1962 by George Matheron, initially developed for ore reserve estimation problems in the mining industry, geostatistics has evolved extremely, including many methods, techniques and approaches for spatial modelling of natural phenomenon in the Earth sciences. From mining, geostatistics has spread and has become an important methodology in many fields of application like petroleum industry, geology, climatology, agriculture, soil science, forestry etc. For these reasons, only a very brief introduction of geostatistics and very basic principles and terms will be given in this section.

Geostatistics provides a wide variety of tools to quantify and model the degree of spatial similarity and spatial variability. The aim of geostatistical methods for modelling of spatial variability is a random variable Z distributed in space and/or time. In geostatistical applications, a random variable is a function of spatial coordinates at any point of the studied area, in which each point $\mathbf{u}$ is determined by geographic (and/or time) coordinates in one, two or three-dimensional space; $\mathbf{u} = (X, Y, Z)$. Set of such random variables at each point $\mathbf{u}$ of the studied domain D represents a random function $Z(\mathbf{u})$. One realization of a random function, or one realization of each random variable in the space, consists of a set of values $z(\mathbf{u})$ called a regionalised variable (Matheron, 1971).

In geostatistical application, a random function $Z(\mathbf{u})$ can be expressed as the sum of two parts (Dowd, 2004):

1. A deterministic part $m(\mathbf{u})$, called *drift* or *trend*, represented by a deterministic function of location (linear, quadratic, etc.).
2. A stationary random function $R(\mathbf{u})$ with a constant mean that represents the deviation from the mean $m(\mathbf{x})$, so called residuals, and can be estimated by the standard techniques of stationary methods.

The above terms yield to the following expression of the random function $Z(\mathbf{u})$:

$$Z(\mathbf{u}) = R(\mathbf{u}) + \underbrace{m(\mathrm{u})}_{\mathrm{E}[Z(\mathbf{u})]} . \tag{1}$$

If we assume that the mean $m(\mathbf{u})$ is constant, then we have the basis for the geostatistical methods of overcoming the problems imposed by stationarity. A decision of stationarity of available data used for spatial modelling is necessary for all geostatistical modelling. However, as stated by Journel (1986), stationarity is a constitutive property of the random function and not an intrinsic property of the studied phenomenon and therefore a decision about stationarity is, in fact, a model itself.

2.1 Variogram

The variogram is the basic structural tool to model spatial continuity in geostatistical applications. It represents bivariate statistics, which express the variability of increments of the values z of random variables Z at points $\mathbf{u}$ separated by a vector $\mathbf{h}$. This direct variogram can be expressed as follows:

$$\begin{aligned} 2\gamma_Z(\mathbf{h}) &= \mathrm{E}\left[\left\{ Z(\mathbf{u}) - Z(\mathbf{u}+\mathbf{h}) \right\}^2 \right] \\ &= 2\left[\mathrm{C}(0) - \mathrm{C}(\mathbf{h}) \right], \end{aligned} \tag{2}$$

where $\mathrm{C}(\mathbf{h})$ represents covariance between $Z(\mathbf{u})$ and $Z(\mathbf{u} + \mathbf{h})$ with constant mean m and $\mathrm{C}(0) = \mathrm{Var}[Z(\mathbf{u})] = \sigma^2$ represents apriori variance of $Z(\mathbf{u})$.

The expression (2) simply describes how the values of Z at two points $\mathbf{u}$ and $\mathbf{u} + \mathbf{h}$ become different as the separation vector $\mathbf{h}$ between pairs of points increases. Graphically, the variogram is a positive function increasing with $\mathbf{h}$ and it describes the change of the spatial variability of the studied features in the studied area for any distance and any direction of space (Armstrong, 1998).

The final model of the variogram describes the change of the spatial variability and, consequently, it is used in the geostatistical modelling. The main role of geostatistics is to make an estimation of the unknown value at unsampled locations.

2.2 Kriging

The geostatistical estimation procedure is called kriging, developed by George Matheron in 1963, and it is named in honour of Daniel G. Krige, following his university thesis. Nowadays, under kriging we understand "a collection of generalized linear regression techniques for minimizing an estimation variance" (Olea, 1991) that is used to estimate unknown values at unsampled locations using surrounding

data $z(\mathbf{u}_\alpha)$. It is beyond the scope of the paper to present all different kriging techniques due to their wide variation. The paper present the general model named universal kriging (UK) (Matheron, 1971) assumes that the mean in (1) can be written in a form of finite polynomial of order K, or trend, in practise of first or second order:

$$m(\mathbf{u}) = \sum_{k=0}^{K} a_k \mathbf{u}^k. \tag{3}$$

Since kriging is a method of a linear regression, a weighted linear estimator at unsampled location $\mathbf{u}_o$ in the stationary case where the mean m is known can be written as:

$$z^*(\mathbf{u}_o) - m = \sum_{\alpha=1}^{n(\mathbf{u}_o)} \omega(\mathbf{u}_\alpha)\big(z(\mathbf{u}_\alpha) - m\big) \quad \text{or shortly} \quad z_o^* = \sum_{\alpha=1}^{n_o} \omega_\alpha \underbrace{(z \quad - m)}_{\text{residuals } r_\alpha} \tag{4}$$

where ω_α are the weights assigned to the n_o data z_α within a search neighbourhood available for estimation. The estimation variance for universal kriging is given by (Dowd, 2004):

$$\sigma_e^2 = \mathrm{Var}\left[Z_o^* - Z_o\right] = 2\sum_{\alpha=1}^{n_o} \omega_\alpha \gamma_{\alpha o}^R - \sum_{\alpha=1}^{n_o}\sum_{\beta=1}^{n_o} \omega_\alpha \omega_\beta \gamma_{\alpha\beta}^R - 2\sum_{k=0}^{K} \lambda_k \left(\sum_{\alpha=1}^{n_o} \omega_\alpha \mathbf{u}_\alpha^k - \mathbf{u}_o^k \right), \tag{5}$$

with sample-to sample variogram of residuals $\gamma_{\alpha\beta}^R$, sample-to-target variogram $\gamma_{\alpha o}^R$ and a set of Langrange multipliers λ_k for a given trend order K.

The weights ω_α in equation (4) are derived by minimizing of the estimation variance (5) and solving a kriging system of linear equation:

$$\begin{cases} \sum_{\beta=1}^{n_o} \omega_\beta \gamma_{\alpha\beta}^R + \sum_{k=0}^{K} \lambda_\alpha^k f_\alpha^k = \gamma_{\alpha o}^R \quad \forall \alpha\,, \\ \sum_{\alpha=1}^{n_o} \omega_\alpha f_\alpha^k = f_o^k \quad \forall k\,. \end{cases} \tag{6}$$

Associate kriging variance, independent of available data values, becomes:

$$\sigma_K^2 = \sum_{\alpha=1}^{n_o} \omega_\alpha \gamma_{\alpha o}^R - \sum_{k=0}^{K} \lambda_k \mathbf{u}_o^k. \tag{7}$$

2.3 Geostatistical simulation

The aim of kriging is to produce the best accurate estimation of the mean value of a random variable Z at an unsampled location $\mathbf{u}_o$, $E[Z(\mathbf{u}_o)]$ in the sense of the least-square method because of minimizing the local estimation variance σ_e^2. The spatial structure of the estimated values differs from that of the actual ones (de Fouquet, 1993). The map of kriged estimates is interpreted as a set of expectations of the random variables at all locations $\mathbf{u}_o$ and tends to smooth out the local variability of the data. That means that low values are overestimated whereas high values are underestimated. The smoothing effect of kriging is a serious disadvantage when trying to reproduce the extreme values. One important fact is that the smoothing effect of kriging depends on the data location – smoothing is smaller close to the data location and conversely. The final kriged map is therefore less variable than the data.

Stochastic simulation produces the maps of realisations $z_s(\mathbf{u}_o)$ of a set of random variables $Z(\mathbf{u}_o)$ at all unsampled locations $\mathbf{u}_o$. The aim of the simulation is to randomly draw several realisations of the random function that reflect the variability of the sample values (data histogram and variogram). Each simulated realisation represents a possible version of reality coherent with the data values and a used model of variability as well. A simulation that does not honour the experimental data values is called non-conditional simulation (NS). There are many methods for generating a realisation of the non-conditional simulation (for example sequential methods, spectral methods, LU covariance matrix decomposition, turning bands, etc.). Each method has its own advantages and disadvantages, as may be seen for example in Chilès and Delfiner (1999) or Lantuéjoul (2002). In general, non-conditional simulation is one possible realisation of a random function that has the same variogram model as the one modelled from the sample data, but it is otherwise totally unrelated to them (Chilès and Delfiner, 1999). Non-conditional simulation is conditioned by kriging. Conditioning is a process by which we can pass from a non-

conditional simulation Z_{NS} to a conditional simulation Z_{CS} that match the sample points $z(\mathbf{u}_\alpha)$ of random function $Z(\mathbf{u})$. Non-conditional and conditional simulations are independent, but with the same input variogram model. Conditional simulation $Z_{CS}(\mathbf{u})$ is built by adding of the kriging error $[Z(\mathbf{u}) - Z_K^*(\mathbf{u})]$ to the kriging estimation $Z_K^*(\mathbf{u})$. However, the kriging error is unknown because $Z(\mathbf{u})$ is not known. Therefore the kriging variance is replaced by non-conditional simulation of the kriging variance $[Z_{NS}(\mathbf{u}) - Z_{NS}^*(\mathbf{u})]$ where non-conditional simulation $Z_{NS}(\mathbf{u})$ is known on a simulated grid and is based on the variogram modelled from the sample data. Estimation of the non-conditional simulation $Z_{NS}^*(\mathbf{u})$ is based on kriging of the values of the non-conditional simulation at the sample locations $\mathbf{x}_\alpha$ using the same variogram model.

A set of L independent and equal probable realisation of random function from conditional simulation constitutes a numerical model. Simulation post-processing and ranking of the realisations from the smallest realisation to the largest one enables to construct an inverse distribution curve for any single cell of simulated grid, a group of cells or the entire area under consideration. The curve represents a probability, or risk curve.

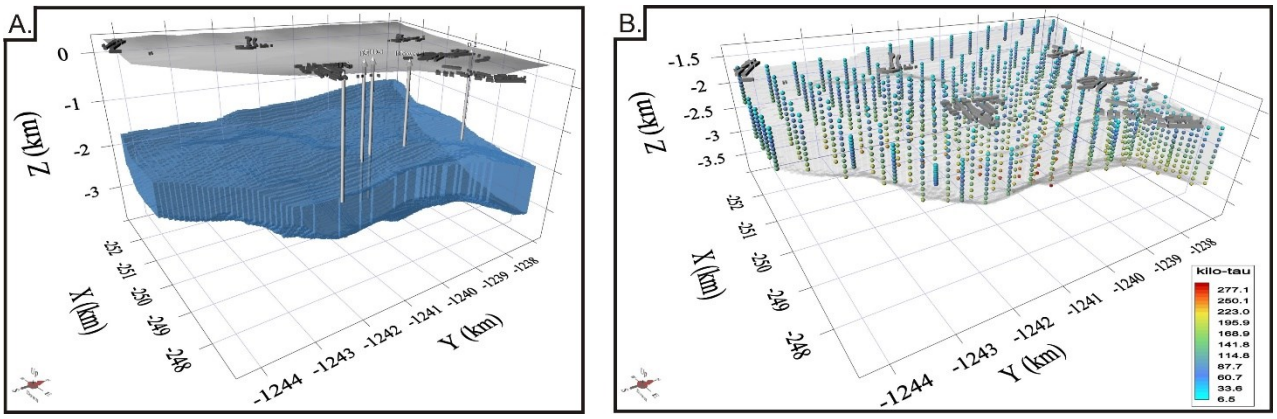

Figure 2: 3D grid of Ďurkov hydrothermal reservoir (A.) and spatial arrangement of 1650 calculation points within (B.).

The Turning Band (TB) algorithm was selected for studied variables simulation. It was the earliest algorithm for simulation of autocorrelated random processes in two or three dimensions (Deutch and Journel, 1998). The principle is to produce a non-conditional simulation that reflects the variogram structure but does not honour the input data. Independent one-dimensional realisations are first simulated along lines radiating from central points. Then, each point in 3D space is orthogonally projected into every line and the simulated values nearest to the projected points are averaged. The non-conditional simulation is then conditioned by kriging, which is used to interpolate the experimental error between data and non-conditional simulated values at the data points. The TB algorithm is suitable for all covariance models, does not assume Gaussian type model (Chilès and Delfiner, 1999) and it is great compromise between quality and computing time.

3. INPUT DATA

Creation of final model begins with a primary reservoir body dissection into 150 points regularly spaced of 500x500 m located on the top surface of the reservoir. Then, the reservoir was vertically divided into proportionally distributed 10 sublayers according to an overall reservoir thickness at given point on top reservoir surface. Thus, the studied hydrogrothermal reservoir Ďurkov was subdivided into 1650 points **u** in total (Figure 2, B.) for calculation of the studied convention indicators.

The calculation points served to calculate reservoir matrix and fluid parameters prior processing in a refined 3D 50 x 50 x 10 m stabled-surface model with more than 1.4 million grid nodes for using of geostatistical simulations to create a numerical models of variables under study (Figure 2, A.). To study plausibility of reservoir convection, we decided to follow a Linear Stability Analysis concept in combination with the Rayleigh number *Ra* and overheat ratio τ application.

The Rayleigh number *Ra* [–] is a dimensionless vigour on a buoyancy forces applied to a geothermal reservoir media in a ratio to the viscous forces (Bories & Combarnous, 1973). It assumes the uniform heating at a base of the porous environment. Because of horizontally bedded porous media concept applied, this study does not account for reservoir inclination to the impact of a gravity field (Rabinowicz et al., 1999; Pasquale et al., 2013; Lipsey et al., 2016). For the presented paper, it is not necessary to express Rayleigh number calculation because of its complexity. The important thing that the Rayleigh number is function of temperature T as well as the terms used for its calculation as the coefficient of thermal expansion α_{vw}, reservoir fluid density ρ_w, heat capacity c_w and dynamic viscosity v_D. That will affect the following steps in the spatial modelling as an exploratory data analysis, variography or simulation itself.

The critical Rayleigh number for the onset of free, temperature driven convection is Rc = 39,5, so that the creation of convection cells may be expected when $Ra \geq 39.5$. This is, however, a valid condition for uniformly heated (Hanano & Kajiwara, 1999) porous media.

Due to the distribution of formation temperatures at the studied structure, the overheat ratio τ concept (8) is applied (Hanano, 1998), comparing top and bottom thermal conditions to expected steady conductive distribution. The ratio, thus, compensates for non-uniform heat increment to the reservoir (9):

$$\tau = \frac{T_{i+1} - T_i}{T_{i+1}} \quad [-] \tag{8}$$

$$Rc = 38.71e^{-4.176\tau} \quad [-] \tag{9}$$

We can see from the above expression (8) that the τ values is nothing than difference between a base temperature T_{i+1} and a top temperature T_i standardized by T_{i+1} to get values between 0 and 1. The calculated values of the overheating ratio τ ranging from 0.00654 to 0.29515 that give us the range of the τ values equal to 0.28861. The calculated values were multiplied by 1000 to "stretch" the range. It prevents of possible underestimation of the τ values and getting negative results. Thus, new τ values ranging from 6.54 to 295.15 with mean value of 98.98. Figure 3 D. shows experimental histogram of calculated τ values at 1650 sample points. The histogram shows skewing toward to the lower values with only approximately 7% values higher than 200.

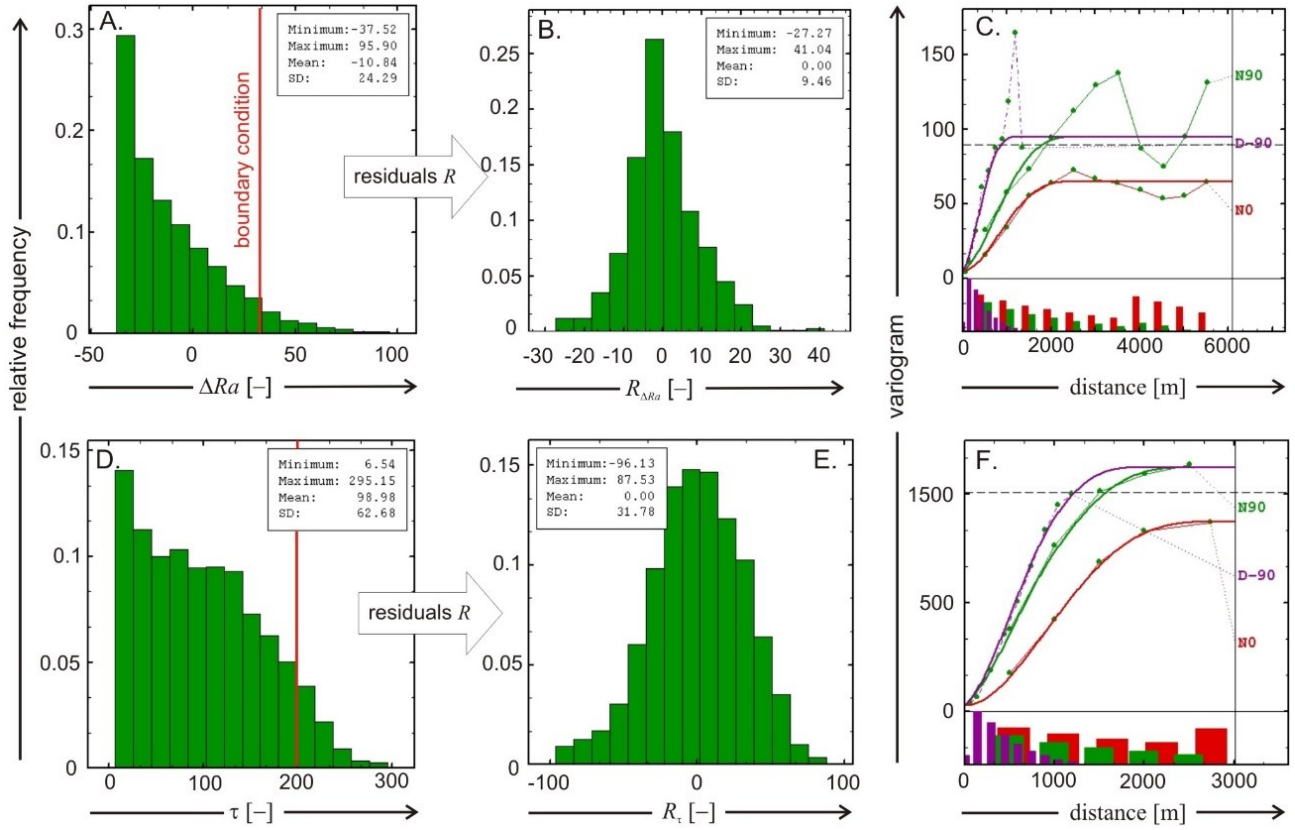

Figure 3: Experimental histogram of raw calculated data (A., D.) their respective histograms of residuals (B., E.) and final variogram models of residuals (C., F.).

The calculated values of Rayleigh number *Ra* ranging from 0.06 to 112 with a mean value 15.61. The critical number *Rc* ranging from 11.29 for τ_{max} to 37.66 for τ_{min} with a mean value 15.61. The final values of calculated Rayleigh number *Ra* and critical Rayleigh numbers *Rc* were used to create a new variable called Δ*Ra* at 1650 point as differences between *Ra* and *Rc*: Δ*Ra* = *Ra* – *Rc*. The Δ*Ra* ranging from -37,52 to 95,9 with mean value -10,84. Respective experimental histogram is shown on Figure 3 A. The histogram is highly skewed toward to lower values with less than 30% values positive values higher than 0.

4. RESULTS AND DISCUSSION

As a matter of fact, the calculated variables τ and *Ra*, and thus Δ*Ra*, described in section 3, are function of temperature, which is, in fact, function of depth. It can be seen on Figure 2, B. where the τ values at the calculation points are shown in coloured scale with obvious tendency Therefore, a non-stationary model was considered during spatial modelling phase under assumption of systematic increasing the values of studied variables with depth in vertical direction. To build the non-stationary model, the first step consisted in modelling a trend

function by means of the least square polynomial method fitting. Under assumption of stationarity in a horizontal plane XY; a linear model in form of $m(Z) = a_0 + a_1 Z$ was fitted to obtain a stationary residual variables $R_{\Delta Ra}(\mathbf{u}_\alpha)$ and $R_\tau(\mathbf{u}_\alpha)$ The final residuals follow a normal distribution with zero means (Figure 3 B and E, respectively).

The experimental variograms were calculated for the residual variables: two experimental variograms in N-S and E-W directions in horizontal planes with lag distance 500 m in accordance with the sample spacing, and one experimental variogram in vertical direction. Nested basic structures of spatial variability were fitted to the directional experimental variogram to build variogram models. The final variogram models of calculated residuals are shown in Figure 3 C for $R_{\Delta Ra}$ and Figure 3 F for R_τ. Both variogram models perfectly fit the directional experimental variograms with low nugget effect values and parabolic behaviour at the origins of models. They also exhibit a strong anisotropical pattern with apparent zonal anisotropy in horizontal plane prolonged in N-S direction, coincident with reservoir body and direction of main geological faults, and vertical direction toward the north, which is in accordance with stratified structure of the calculated variables under study. There is also presence of geometrical anisotropy between E-W and vertical directions and with higher continuity in E-W, which indicates the lowest continuity of studied variables in vertical direction, higher continuity in E-W direction and the highest continuity in N-S direction. By adding the variogram models of residual variables to the linear trend model initialized at the trend modelling stage, the required non-stationary models are obtained and used during geostatistical simulations.

Simulated grid consisted of more than 1.4 million grid nodes on a three-dimensional regular grid 50 x 50 x 10 m with the total volume more than 35 milliards m^3. One hundred of realizations in total were simulated by Turning Bands method using a given model variogram and search neighbourhood. Non-conditional simulations were conditioned by universal kriging due to using non-stationary structural model.

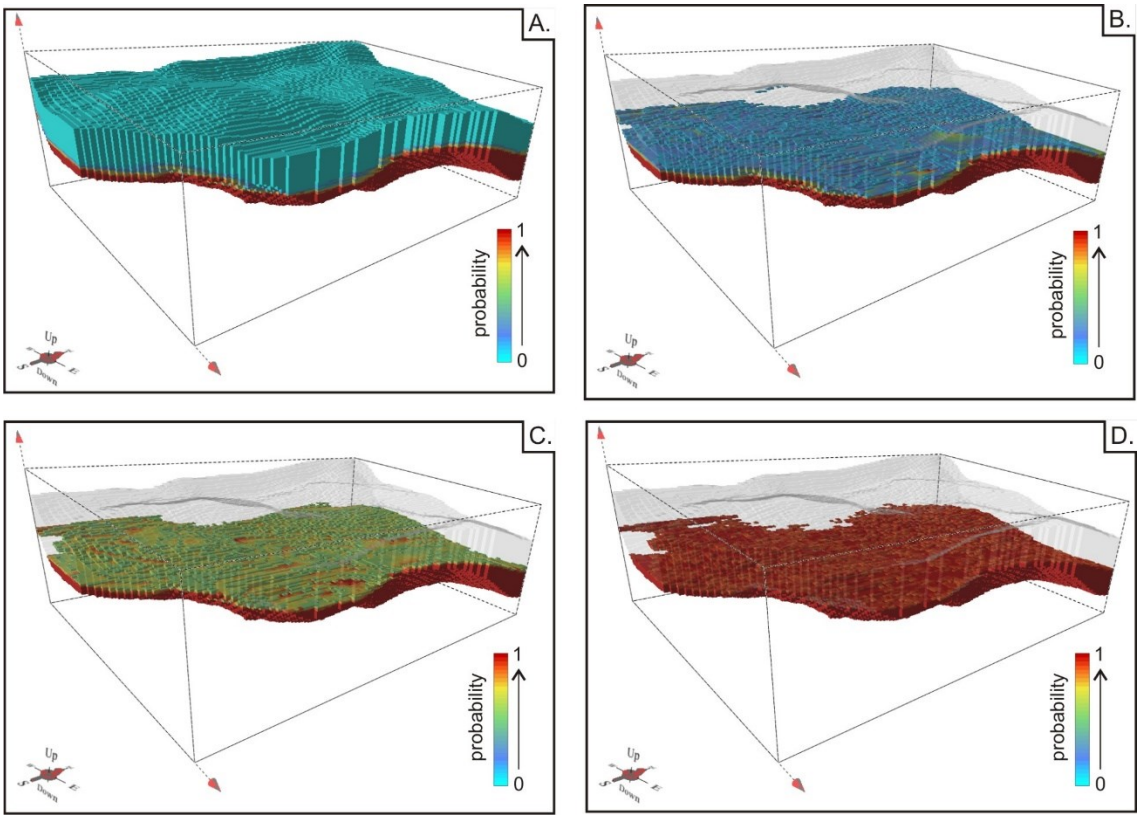

Figure 4: Probability model of positive ΔRa (A.) with extracting the probabilities lower than 0.1 (B.), 0.5 (C.) and 0.9 (D.).

The final numerical model consists of 100 simulated reservoir bodies filled by simulated values of ΔRa and τ. The individual simulations of the numerical model slightly exceeded experimental minimal and maximal values observed from the input data for both studied variables due to using non-stationary modelling approach. It is well know that non-stationary approach often exceeds input data range mainly in extrapolation areas of studied domain. The maximum values for the individual simulations of numerical model are well reproduced.

Simulation post-processing consists in splitting each of 100 realization into two parts – above and below of a boundary condition: 0 for ΔRa and 200 for τ. On the grid node basis, post-processing continues with counting the number of times when the simulated values of each realization exceed the boundary condition. This number above boundary condition is normalized by total number of simulations to obtain probability values ranging from 0 to 1.

Figure 4 A. shows probability model for $\Delta Ra \geq 0$. As can be seen on the figure, there is very tight transition in vertical direction among very low probabilities in the upper part of reservoir and the very high probabilities underneath it. The Figures 4 B., C. and D. show different reservoir proportions for positive ΔRa being above the probabilities 0.1, 0.5 and 0.9 respectively. It can be seen decreasing tendency in total reservoir volume with increasing probability. For instance, only 37% of total volume gains probability more than 0.1. Similarly, there is only 31% of total reservoir volume with probabilities more than 0.5 and only 26% with probabilities more than 0.9. The probability curve of reservoir volume in millions m^3 [Mm^3] is shown in Figure 6 A. Probable volume of the reservoir for positive values of ΔRa ranging from 10,870 Mm^3 to 11,483 Mm^3 with average volume about 11,127 Mm^3, which correspond to approximately one third of the total reservoir volume fulfilling the boundary condition $\Delta Ra \geq 0$.

Figure 5 A. shows probability model for $\tau \geq 200$. The highest probabilities are located at the very bottom part of the reservoir, mainly in the eastern part, with continuity direction NNE–SSW. The Figures 5 B., C. and D. show different reservoir proportions for $\tau \geq 200$ being above the probabilities 0.1, 0.5 and 0.9, respectively. There is only 14% of total reservoir volume with probabilities above 0.1, decreasing to 9% for probabilities above 0.5, and less than 6% with probabilities above 0.9. The probability curve of reservoir volume in millions m^3 is shown in Figure 6 B. Probable volume of the reservoir for $\tau \geq 200$ ranging from 2,974 Mm^3 to 3,760 Mm^3 with average volume about 3,350 Mm^3, which correspond from 9 to 11% of the total reservoir volume fulfilling the boundary condition.

A steady-state pre-production model has been used to analyse sources, plausibility and extension of reservoir overheating (a closed-system model) and convection formation (linear stability analysis). At a given overheating ratio range τ local highs of $\tau \geq 200$ locate in the eastern part of the reservoir at depths of 2,800-4,000 m, however, 90 % probability of $\tau \geq 200$ is fairly reduced to depths below 3,500 m, which haven't been drilled yet. A conditional simulation yields fining upwards trend in overheat. Lateral allochtonous heat sources are missing at the site, implying a tectonics-controlled overheating at contacts between dissected Mesozoic blocks of different uplift tendencies, so that the heat flux to the base or at walls is distributed unevenly. A trail-off overheating trend eastward from the Ďurkov tectonic block towards Neogene volcanics, preserving only fining-upwards profile limits their impact on recent thermal field regime in the reservoir.

The zone with positive ΔRa has been identified at depths below 2,500 m, following a same distribution as the overheat ratio does. There is, thus, a possibility for convection formation in deeper parts of the system. If it is so, convection cells may form individually, bound to particular tectonic blocks, with uplift zones along faults that dissect the reservoir facies, whereas downflow realizes through connected karstified channels in the rock. Convective heat and mass flux may be even more promoted where discontinuities intercept and fissure or matrix permeability is, obviously, increased.

Out of the entire reservoir, the highest plausibility for convection creation is the polygon between towns of Ďurkov – Olšovany and Svinica – Bidovce (Figure 1). Still, presented approach follows the concept of horizontally bedded strata. Tectonic dissection itself, however, expects application of inclined porous media approach, and so to introduce an angle of tilt into critical Rayleigh number analysis to account on a detailed reservoir geometry. This is a topic for the future research.

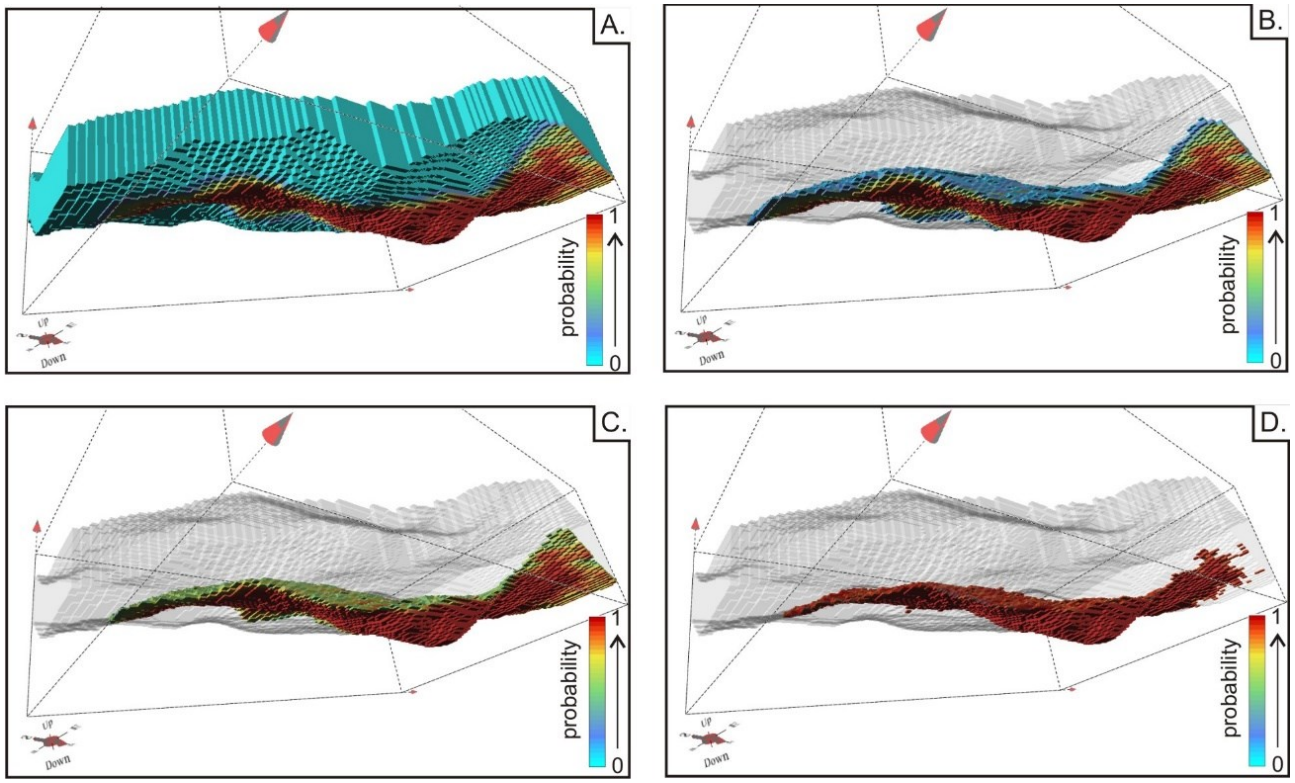

Figure 5: Probability model of τ (A.) with extracting the probabilities lower than 0.1 (B.), 0.5 (C.) and 0.9 (D.).

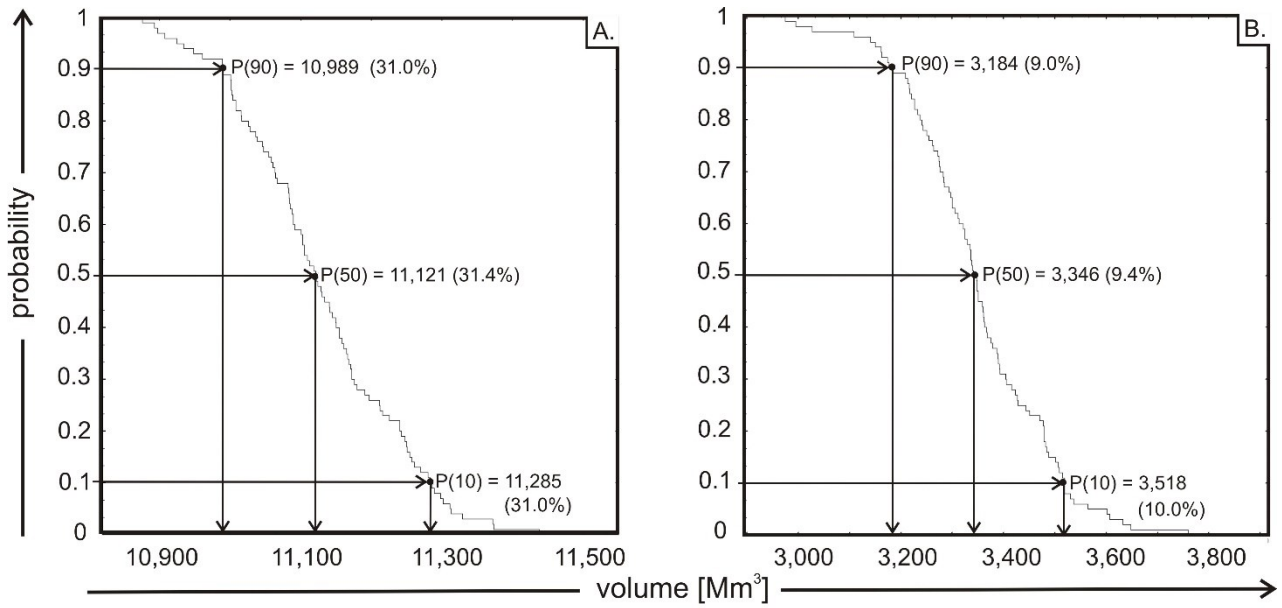

Figure 6: Volumetrics risk curves for studied variables ΔRa (A.) and τ (B.).

5. CONCLUSION

Understanding reservoir heat and mass flux mechanisms is key in setup of reservoir response and reservoir chemistry models. The Ďurkov hydrogeothermal structure, as a low to moderate enthalpy closed system, was assumed purely conductive environment. Although thermal diffusion prevails clearly, overheat-modified linear stability analysis shows that even under conductive profile, limited convection cells may form, not compromising the basic concept of the entire geothermal play-type. The presented paper deals with a methodology allowing for identification of convection indicators for given boundary conditions in a probabilistic framework using geostatistical simulations. Carried simulations show that the most plausible zone for convection formation extend at greater depths that those already drilled, below 3,500 m. Now let us assume that the critical permeability is enhanced along tectonic systems. Yet at given Rayleigh number, the convection appears concentrated into a few insulated cells with very limited vertical extent. Then, with upwards-fining temperature gradient, the velocity of upflow is expected to slow so that viscous forces prevail and slow cooling takes part. Consequently, with decreasing upflow velocity, the rate of pressure and temperature change decreases, limiting boiling processes. Although evaded, most of a gas condensates during a rise or is saturated into a reservoir media. Limitation of the only natural process of gas cap formation points to an artificial origination of the cap. Indeed, high CO_2 content potentially forming the cap is, thus, resultant to deep geological drilling in 70's, during a country-wide prospection on natural gas and oil.

REFERENCES

Armstrong, M.: *Basic Linear Geostatistics*. Springer (1998) ISBN-10 3-540-61845-7.

Bories S.A. and Combarnous M.A.: Natural convection in a sloping porous layer, Journal of Fluid Mechanics, 57 (1), (1973), 63-79.

Bodvarsson G.S., Benson S.M. and Witherspoon P.A.: Theory of the development of geothermal systems charged by vertical faults, Journal of Geophysical Research, 87 (B11), (1982), 9317-9328.

Chilès, J. and Delfiner, P.: *Geostatistics: Modelling Spatial Uncertainty*. John Wiley and Sons, Inc. New York. (1999) ISBN 0-471-08315-1.

Clark, I. and Harper, W. V.: *Practical Geostatistics 2000*. Greyden Press, U.S.A. (2000) ISBN 0-9703317-0-3.

de Fouquet, C.: Reminders on the conditioning kriging. In: *Geostatistical simulations pp 131–145.* Edited by Armstrong M, Dowd, P., A. Kluwer Academic, Dordrecht, (1993).

Deutsch, C., V. and Journel, A., G.: *GSLIB Geostatistical Software Library*. 2nd edition. Oxford University Press Inc. New York. (1998) ISBN 0-19-510015-8.

Dowd, P., A.: *MINE5260 Non-Stationarity*. MSc. in Mineral Resources and Environmental Geostatistics. University of Leeds, Leeds. 2004. U.K (2004).

Fričovský B., Vizi, L., Gregor, M., Zlocha, M., Surový, M. and Černák, R.: Thermodynamic Analysis and Quality Mapping of A Geothermal Resource at the Ďurkov Hydrogeothermal Structure, Košice Depression, Eastern Slovakia. Proceedings, 43rd Workshop on Geothermal Reservoir Engineering Stanford University, Stanford, CA, (2018).

Goovaerts, P.: *Geostatistics for Natural Resources Evaluation*. Oxford University Press, Inc. 1997. London. (1997) ISBN 0-19-511538-4.

Hanano M., 1998: A simple model of two-layered high-temperature liquid-dominated geothermal reser-voir as a part of large-scale hydrothermal convection system, Transport in Porous Media, 33, (1998), s. 3-27.

Hanano M. and Kajiwara T., 1999: Permeability associated with natural convection in the Kakkonda Geothermal Reservoir, Geothermal Resources Council Transactions, 23, (1999), 351-360.

Isaaks, E., H. and Srivastava, R., M.: *An Introduction to Applied Geostatistics*. Oxford University Press, Inc. New York. (1989) ISBN 0-19-505013-4.

Journel, A., G. and Huijbregts, C., J.: *Mining Geostatistics*. Academic Press, Inc. London. (1978) ISBN 0-12-391050-1.

Journel, A., G.: Geostatistics: Model and Tools for the Earth Sciences. *Mathematical Geology, Vol. 18, No. 1, pp 110 – 130*. (1986)

Kassoy D.R. and Zebib A., 1975: Variable viscosity effects on the onset of convection in porous media, The Physics of Fluids, 18 (12), (1975), 1649-1651.

Kühn M., Dobert F. and Gessner K.: Numerical investigation of the effect of heterogeneous permeability distributions on free convection in the hydrothermal system at Mount Isa, Australia, Earth and Planetary Science Letters, 244, (2006), 655-671.

Lantuéjoul, Ch.: *Geostatistical Simulations. Models and Algorithms*. Springer-Verlag Print, Berlin. (2002) ISBN 3-540-42202-1.

Leuangthong, O., Khan, K., D. and Deutsch, C., V.: *Solved problem in geostatistics*. John Wiley and Sons, Inc.. New Jersey. (2008) ISBN 978-0-470-17792-1.

Ledru P. and Gillou-Frottier L.: Reservoir definition. In: Huenges, E. (Ed.): Geothermal Energy Systems. Exploration, Development and Utilization. Wiley-VCH Verlag, Weinheim, DE, (2010), 1-37.

Lipsey, L., Pluymaekers, M., Goldberg, T., van Oversteeg, K., Ghazaryan, L., Cloetingh, S. and van Wees J.-D.: Numerical modelling of thermal convection in the Luttelgeest carbonate platform, the Nederlands, Geothermics, 64, (2016), 135-151.

Matheron, G.: Principles of Geostatistics. *Economical Geology pp. 1246–1266*. Vol. 58. (1963).

Matheron, G.: *The theory of regionalized variables and its application.* Les Cahiers du Centre de Morphologie Mathématique. École Nationale Supérieure des Mines Paris. Fontainebleau, Paris, France. (1971)

Olea, R., A.: *Geostatistical Glossary and Multilingual Dictionary*. Oxford University Press, Inc. (1991) ISBN 0-19-506689-9.

Olea, R., A.: *Geostatistics for Engineers and Earth Scientists*. Kluwer Academic Publishers. (1999) ISBN 0-7923-8523-3.

Pasquale V., Chiozzi P. and Verdoya M., 2013: Evidence for thermal convection in the deep carbonate aquifer of the eastern sector of the Po Plain, Italy, Tectonophysics, 594, (2013), 1-12.

Pereszlenyi M., Pereszlenyiova A. and Masaryk P.: Geological setting of th Košice Basin in relation to geothermal energy resources, Bulletin d'Hydrogéologie, 17, (1999), 1-8.

Rabinowicz M., Sempéré J-Ch. and Genthon P., 1999: Thermal convection in a vertical permeable slot: Implications for hydrothermal circulation along mid-ocean ridges, Journal of Geophysical research, 104 (B12), (1999), 29275-29292.

Ravenscroft, P., J.,: Conditional Simulation for Mining: Practical Implementation in an Industrial Environment. In *Geostatistical Simulations*. Armstron, M.; Dowd, P., A.(Eds.). Pp. 79 – 89. Kluwer Academic Publishers. (1994) ISBN 0-7923-2732-2.

Tóth A.N.: Heat losses in geothermal reservoir, Geosciences and Engineering, 1 (2), (2012), 321-327.

Wackernagel, H.: *Multivariate Geostatistics*. 3rd edition. Springer-Verlag Print, Berlin. (2003) ISBN 3-540-44142-5.

Wang C.T. and Horne R. N.: Boiling flow in horizontal structure, *Geothermics*, **29**, (2000), 759-772.Wang C.T. and Horne R. N.: Boiling flow in horizontal structure, *Geothermics*, **29**, (2000), 759-772.

Webster, R. and Oliver, M., A.: *Geostatistics for Environmental Scientists*. John Wiley and Sons, Inc. 2001. New York. (2001) ISBN 0-471-96553-7.